

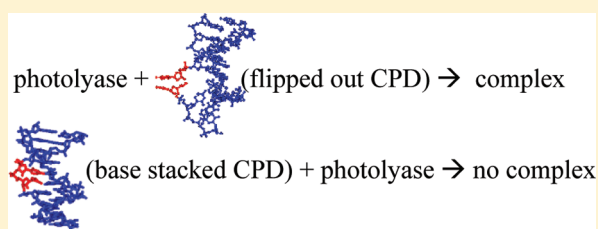
Evidence from Thermodynamics that DNA Photolyase Recognizes a Solvent-Exposed CPD Lesion

Thomas J. Wilson, Matthew A. Crystal,[†] Meredith C. Rohrbaugh, Kathleen P. Sokolowsky,[‡] and Yvonne M. Gindt^{*}

Department of Chemistry, Hugel Science Center, Lafayette College, Easton Pennsylvania 18042, United States

 Supporting Information

ABSTRACT: Binding of a *cis,syn*-cyclobutane pyrimidine dimer (CPD) to *Escherichia coli* DNA photolyase was examined as a function of temperature, enzyme oxidation state, salt, and substrate conformation using isothermal titration calorimetry. While the overall ΔG° of binding was relatively insensitive to most of the conditions examined, the enthalpic and entropic terms that make up the free energy of binding are sensitive to the conditions of the experiment. Substrate binding to DNA photolyase is generally driven by a negative change in enthalpy. Electrostatic interactions and protonation are affected by the oxidation state of the required FAD cofactor and substrate conformation. The fully reduced enzyme appears to bind approximately two additional water molecules as part of substrate binding. More significantly, the experimental change in heat capacity strongly suggests that the CPD lesion must be flipped out of the intrahelical base stacking prior to binding to the protein; the DNA repair enzyme appears to recognize a solvent-exposed CPD as part of its damage recognition mechanism.



INTRODUCTION

One of the most common types of UV-induced damage to DNA is the *cis,syn*-cyclobutane pyrimidine dimer (CPD). The lesion is potentially mutagenic, and a number of repair mechanisms have evolved to protect organisms from this type of damage.¹ One of the simpler proposed mechanisms for repair of the CPD comes from DNA photolyase (PL), a DNA repair enzyme widely found throughout all kingdoms of life with the exception of placental mammals.^{2,3} PL recognizes and binds to the CPD lesion and then uses a light-driven electron transfer to reverse the damage on the DNA. The mechanism of the light-driven electron transfer repair has been well studied, but the mechanism by which the enzyme is able to recognize and bind the CPD damage, uncoupled from the light-driven repair process, is less understood.

PL requires flavin adenine dinucleotide (FAD) cofactor for CPD repair.² In repair, the fully reduced flavin cofactor (FADH^-) donates an electron to the CPD upon excitation with blue light. The lesion spontaneously repairs followed by an electron transfer back to the flavin. PL, as isolated from *E. coli*, is a monomeric 56 kD protein with the flavin cofactor in an inactive neutral semiquinone state (FADH^\bullet). A two-electron oxidized state, FAD, is also observed with the protein. The protein with any of three oxidation states of FAD present is able to bind CPD but is unable to bind CPD if the FAD cofactor is absent.^{4,5} A second chromophore, methenyltetrahydrofolate (MTHF) in *E. coli* PL, is generally present; it may play a role as a light-harvesting pigment with energy transfer to FAD, but it is not required for enzymatic activity.

Several crystal structures have been published for free PL, but only one is available for the enzyme substrate complex with

enzyme from *Anacystis nidulans* along with a CPD analog that is apparently repaired during acquisition of the crystal structure data.^{6–9} In 2002, work by the Stanley group provided evidence that the CPD lesion was flipped out of the base-stacking conformation upon binding to PL,¹⁰ and the crystal structure of the complex later confirmed this conclusion. The adenine ring of the FAD resides 3.1 Å from the bound, repaired CPD, while the isoalloxazine ring of the FAD appears to be within 7 Å of the CPD.⁹ The mechanism by which the CPD is flipped out of the intrahelical DNA and bound to PL is unclear.

One can imagine a number of possible pathways for the binding of the CPD to occur.¹¹ First, as the protein binds to the DNA, it could simultaneously flip out the CPD into a binding pocket as part of the binding interaction. In a second possible pathway, PL could simply recognize a CPD that has spontaneously flipped out of the intrahelical DNA into a solvent-exposed position. Third, as PL binds to the DNA, it could bend the DNA in such a way that it destabilizes the base stacking around the CPD lesion. The lesion is then more likely to flip out to a position where it could be captured by the enzyme. The best characterized base-flipping systems are the DNA glycosylase enzymes in which three forms of the repair enzyme are observed: a search complex that can easily slide along the DNA, an interrogation complex that is able to test the DNA for damaged bases, and an excision complex which is involved in flipping the damaged base out for repair.¹² Upon the basis of its lack of

Received: August 23, 2011

Revised: October 11, 2011

Published: October 22, 2011

similarity to the glycosylase enzymes, it is unlikely that PL follows a similar mechanism; PL lacks a protruding “reading head” for an interrogation complex.¹¹

Interactions between the FAD cofactor and substrate appear to be important since we find the presence of the substrate increases the reduction potential of the $\text{FADH}^-/\text{FADH}^{\bullet}$ couple in PL;¹³ the reduction potential is important for the light-driven repair process. In addition, substrate binding induces changes in both the Raman and the absorption spectra of FADH^{\bullet} ,¹⁴ the neutral semiquinone form of the FAD cofactor that absorbs light from 500 to 650 nm.

The ability to control the oxidation state of a cofactor so close to the binding site allows us to make local modifications immediate to the binding site. In addition, PL is somewhat unusual for a site-specific DNA binding protein in that it has the ability to bind and repair CPD lesions, regardless of the DNA conformation.² To further elucidate the roles of the flavin cofactor and the DNA conformation in the CPD damage recognition mechanism, we completed isothermal titration calorimetry studies (ITC) to measure the thermodynamics of substrate binding to PL.^{15–17} We examined substrate binding as a function of temperature, oxidation state of FAD, salt concentration, and substrate conformation. In addition, we examined the role of the MTHF cofactor in binding. Given the large quantities of substrate required for these studies, our single-strand DNA substrate (ssDNA) is UV irradiated p(dT)₁₀ with an average of one CPD dimer randomly distributed per strand.¹⁴ Our double-stranded substrate is the UV-p(dT)₁₀ titrated with p(dA)₁₀, also with one lesion per unit.

■ EXPERIMENTAL METHODS

Chemicals and Enzyme Used in Experiments. PL was purified as previously described.¹⁸ The enzyme was stored as the semiquinone at -80°C in 20 mM potassium phosphate, 0.400 M K₂SO₄ (storage buffer) at pH 7.0. Undamaged p(dT)₁₀ and p(dA)₁₀ were obtained from TriLink Biotechnologies and used without further purification. The UV-damaged single-strand and double-strand substrates were produced as described earlier after dissolution of the DNA into the appropriate buffer.¹⁴ All other chemicals used were obtained from Sigma-Aldrich.

Preparation of Samples for Temperature-Dependent Binding Studies. The semiquinone enzyme, in the storage buffer, was diluted to $\sim 30 \mu\text{M}$ using appropriate buffer to reach a final buffer composition of 20 mM potassium phosphate and 88 mM K₂SO₄ (Buffer A, $\mu = 300 \text{ mM}$) at pH 7.0. The semiquinone samples for ITC were made fresh each day and stored on ice until use.

Samples with fully reduced enzyme were prepared using three cycles of dilution into Buffer A followed by centrifugal concentration (Amicon Ultra, 30 kD cutoff). The protein was diluted to $\sim 35 \mu\text{M}$ and reduced using the procedure described earlier.¹⁹ Samples were removed for ITC experiments immediately prior to the start of the experiment, while the rest of the reduced enzyme was kept anaerobic on ice.

Samples with fully oxidized enzyme were prepared by diluting the semiquinone protein to $\sim 35 \mu\text{M}$ in Buffer A along with a 25 molar excess of potassium ferricyanide. The sample, in a capped quartz cuvette, was placed on ice and illuminated with white light (2 in. from Philips F20T12 20 W fluorescence light) for 20 min. The absorption spectrum of the sample was measured to ensure there was complete loss of the semiquinone state. The protein

was then exchanged into fresh Buffer A using a small desalting column (Bio-Rad 10 DG) and concentrated using a centrifugal concentrator. Oxidized enzyme was prepared fresh and stored on ice for each day of experiments.

Preparation of Samples for Ionic Strength-Dependent Binding Studies. The solutions, all at pH 7.0 with 50 mM Hepes ($\mu = 12 \text{ mM}$), used to obtain the salt concentration data were as follows: 188 mM KCl ($\mu = 200 \text{ mM}$), 238 mM KCl ($\mu = 250 \text{ mM}$), 263 mM KCl ($\mu = 275 \text{ mM}$), 288 mM KCl ($\mu = 300 \text{ mM}$), 313 mM KCl ($\mu = 325 \text{ mM}$), 338 mM KCl ($\mu = 350 \text{ mM}$), 388 mM KCl ($\mu = 400 \text{ mM}$), and 488 mM KCl ($\mu = 500 \text{ mM}$). The semiquinone protein was diluted and concentrated (three cycles, Amicon Ultra, 30 kD cutoff) into the appropriate buffer prior to use. The reduced and oxidized forms, prepared as described above, were exchanged into the appropriate buffer using a small desalting column and then concentrated using centrifugal concentrators.

Preparation of Samples for Proton Ionization Studies. The four buffers, all at pH 7.0 with 88 mM K₂SO₄, used in this study were as follows: 20 mM potassium phosphate ($\Delta H_{\text{ion}} = 1.22 \text{ kcal/mol}$), 20 mM Hepes ($\Delta H_{\text{ion}} = 5.02 \text{ kcal/mol}$), 20 mM Mops ($\Delta H_{\text{ion}} = 5.29 \text{ kcal/mol}$), and 20 mM imidazole ($\Delta H_{\text{ion}} = 8.75 \text{ kcal/mol}$).^{20,21} The semiquinone protein was exchanged into the appropriate buffer using a small desalting column (Bio-Rad 10 DG) and concentrated using a centrifugal concentrator. The reduced and oxidized forms, prepared as described above, were exchanged into the appropriate buffer and concentrated as described above.

Activity Assay. The activity of PL was measured using the procedure described earlier¹⁹ with the modifications described below for the fully oxidized state. Oxidized PL ($750 \mu\text{L}$ of $\sim 15 \mu\text{M}$ in Buffer A) was purged for 10 min with N₂ gas at 4°C in a quartz cuvette equipped with a septum. A solution of sodium dithionite (10 mg/mL) was purged for 5 min with N₂ gas. Sodium dithionite (30 μL) was added to the anaerobic PL solution, and the solution was allowed to stand at 25°C until complete reduction of the PL was observed using UV-vis absorption spectroscopy. Fully reduced enzyme was then added to an anaerobic solution of UV-p(dT)₁₀, and the rest of the activity assay was carried out as described previously.¹⁹

Isothermal Titration Calorimetry Measurements. Binding studies were completed with a MicroCal ITC₂₀₀ microcalorimeter (GE Biosciences) at 25°C , unless otherwise noted. PL exchanged into the appropriate buffer and, at concentrations ranging from 25 to 40 μM , was placed in the sample cell. The DNA substrate, in identical buffer, was loaded in the syringe at concentrations ranging from 375 to 500 μM . The substrate was added to the fully reduced enzyme in 19 aliquots ($1 \times 0.4 \mu\text{L}$, $18 \times 2.0 \mu\text{L}$) with 80 s of spacing between each addition, while the other oxidation states were titrated with 24 aliquots ($1 \times 0.4 \mu\text{L}$, $23 \times 1.6 \mu\text{L}$) spaced 90 s apart. The reduced enzyme titration required approximately 35 min, while the other oxidation states required approximately 45 min. Protein and DNA controls were run under identical conditions to correct for simple dilution of the DNA and protein along with any effect of excess sodium dithionite in the reduced enzyme. The protein sample was recovered from the ITC after each experiment, and the absorption spectrum of the solution was measured to determine the concentration of oxidized and semiquinone PL present. Three to ten replicates were completed for each set of experimental conditions.

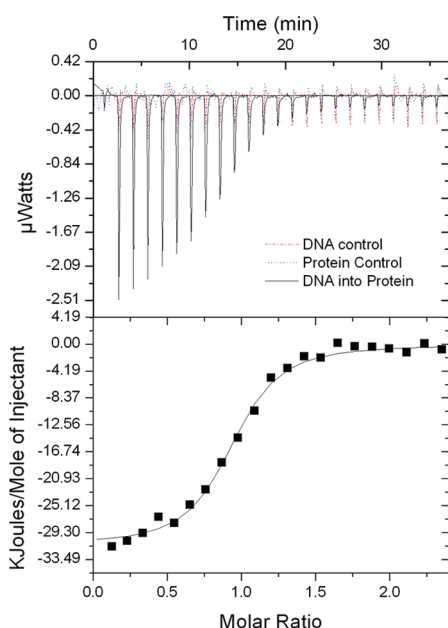


Figure 1. Typical titration of FAD_{ox} with ssDNA and resulting binding curve. The conditions for the ITC shown in panel A were as follows: $[\text{FAD}_{\text{ox}}] = 35 \mu\text{M}$, $[\text{UV-p}(\text{dT})_{10}] = 438 \mu\text{M}$, in 20 mM potassium phosphate, 88 mM K_2SO_4 pH 7.0, $T = 20^\circ\text{C}$. Parameters obtained from the best fit of the binding curve shown in panel B: $N = 0.92 \pm 0.01$, $K_A = 1.0 (\pm 0.1) \times 10^6$, $\Delta H^\circ = -31.3 (\pm 0.6) \text{ kJ/mol}$.

DNA Melt Experiments. The integrity of the double-stranded DNA made from UV-p(dT)₁₀ and p(dA)₁₀ was checked using a DNA melt experiment. The substrate ($10 \mu\text{M}$) in the appropriate buffer was placed in a reduced volume quartz cuvette. The temperature of the sample was controlled using a Peltier cuvette holder in a Cary 50 (Varian) UV-vis spectrometer. The temperature of the solution was changed in 5°C steps (from 5 to 70°C) with an equilibration time of 10 min per step, and the spectrum was measured at each temperature.

Preparation of PL with Stoichiometric Quantities of MTHF Cofactor. Synthetic MTHF was produced as described earlier.²² The MTHF was dissolved in Buffer A and titrated into $\sim 100 \mu\text{M}$ semiquinone PL as described earlier.²² The 360 and 380 nm MTHF absorption bands were monitored to ensure that all of the protein had MTHF bound; unbound MTHF absorbs at 360 nm, while PL-bound MTHF absorbs at 380 nm. The protein with the additional MTHF was diluted to $\sim 35 \mu\text{M}$, and ITC data was obtained with ssDNA at 25°C . Control data were collected on the same day using semiquinone PL from the same preparation in the same buffer.

RESULTS

Integrity of Protein and Substrate Before and After ITC Experiments. Typical ITC data obtained for PL are shown in Figures 1 and 2, showing ssDNA and dsDNA binding, respectively. Figure 1 is an example of the titration of the FAD_{ox} state with ssDNA (UV-p(dT)₁₀). The top panel, Figure 1A, displays the titration of FAD_{ox} with ssDNA along with buffer into FAD_{ox} labeled as protein control, and ssDNA in buffer, labeled as DNA control. The two controls take into account the heat of dilution of protein and substrate. The binding curve generated from the titration, after correcting for the dilution enthalpies, is shown in

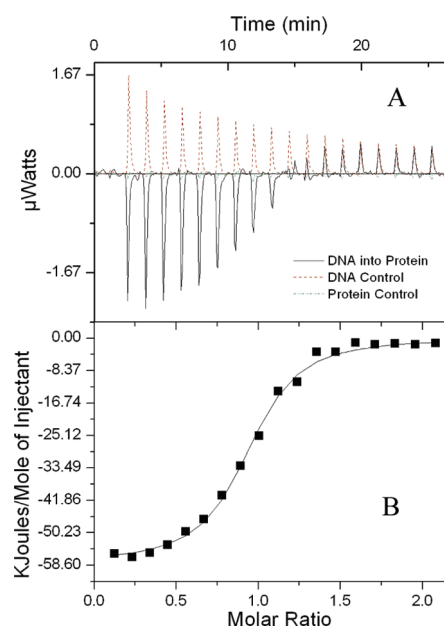


Figure 2. Typical titration of FADH^- with dsDNA and resulting binding curve. The conditions for the ITC shown in panel A were as follows: $[\text{FAD}_{\text{ox}}] = 36.5 \mu\text{M}$, $[\text{dsDNA}] = 375 \mu\text{M}$, in 20 mM potassium phosphate, 88 mM K_2SO_4 , pH 7.0, $T = 15^\circ\text{C}$. Parameters obtained from the best fit of the binding curve shown in panel B: $N = 0.92 \pm 0.01$, $K_A = 1.0 (\pm 0.1) \times 10^6$, $\Delta H^\circ = -57.9 (\pm 0.8) \text{ kJ/mol}$.

Figure 1B. The data fit to a one-site binding model using the propriety software supplied by MicroCal. Figure 2A is typical data obtained for FADH^- titrated with dsDNA (UV-p(dT)₁₀) with a slight excess of p(dA)₁₀) along with the controls for both the PL and the dsDNA alone. The ssDNA control is different from the dsDNA control; the dsDNA control is endothermic, while the ssDNA is slightly exothermic under our buffer conditions. The difference in appearance between our dsDNA and ssDNA controls gives us confidence that our dsDNA is, in fact, double-stranded DNA since dilution of that substrate would be expected to have an endothermic heat of dilution.

While the UV-p(dT)₁₀ substrate with its random CPD location is not optimal for these studies, we believe it is adequate to map out differences in the binding site as the FAD undergoes changes in oxidation state. In general, the number of binding sites for PL binding to both dsDNA and ssDNA is very close to 1; for example, averaging all 44 titrations obtained for the FADH^\bullet state with ssDNA for our temperature study from 10 to 25°C we obtain an average of $0.99 (\pm 0.1)$ binding sites per PL. The number of binding sites decreases slightly (by 0.08) for data at 32 and 37°C ; we ascribe the slight decrease to loss of viable protein rather than to any problem with the ssDNA. In a separate experiment, we monitored the DNA absorbance as a function of temperature and found our dsDNA appeared to melt at $\sim 42^\circ\text{C}$ under the buffer conditions used in the temperature-dependent ITC experiments.

Since we could easily recover the protein after each titration, we also measured the oxidation state of the protein after experiment. Studies at low ionic strengths caused the largest decrease in initial oxidation state with the FADH^- and FADH^\bullet states becoming oxidized over the course of the experiment. In contrast, the FAD_{ox} appeared to be relatively stable under the experimental conditions, though a trace amount of the protein

would precipitate during the experiment. At low ionic strengths we lost less than 15% of the FADH[•] state (to FAD_{ox}) but as much as 45% of FADH⁻ (to FADH[•]). Under the conditions of the temperature study with 20 mM potassium phosphate, 88 mM K₂SO₄ at pH 7.0, PL was more resistant to oxidation with losses of less than 10% and 30% of the FADH[•] and FADH⁻ states, respectively. Each titration took 40–50 min, and we diluted the ITC sample to obtain the absorption spectrum required to determine the oxidation state of the enzyme. The amounts of the reduced PL lost to oxidation, as given above, is most likely an overestimation of the oxidation present during the crucial, initial phase of the binding experiment. We did not attempt to correct for any change in oxidation state during the course of the titration.

We used multiple buffer systems for the work; the buffer and salt present did slightly affect the enthalpies obtained. The temperature studies were completed in 20 mM potassium phosphate, 88 mM K₂SO₄ at pH 7.0 (ionic strength = 300 mM); since the salt studies require a monovalent salt, the buffer was changed to 50 mM Hepes pH 7.0 and KCl to achieve the appropriate salt concentration. For our proton-exchange experiments, we added 88 mM K₂SO₄ cosolvent to 20 mM buffer of known ionization enthalpy (potassium phosphate, Hepes, Mops, imidazole). In addition, we attempted to obtain ITC data using the solvent conditions (10 mM Tris, pH 7.4 with 1 mM EDTA, 1 mM β-mercaptoethanol, 100 μg/mL bovine serum albumin, and 125 mM NaCl) described for earlier binding assays;²³ we were unable to obtain any binding data with this solvent system since the protein almost immediately oxidized to FAD_{ox} from the stable semiquinone state and rapidly precipitated.

Preparation of stable oxidized PL has generally been a problem since the oxidized enzyme tends to precipitate out of solution. We developed a novel preparation that uses excess ferricyanide in the presence of white light to obtain stable oxidized enzyme that is resistant to precipitation; illumination of the semiquinone sample in the presence of the oxidant accelerates the oxidation reaction by an order of magnitude. The mechanism by which the oxidation occurs is unclear, but active protein is recovered upon reduction of the FAD cofactor. The oxidized protein does not survive freeze/thaw cycles well, so oxidation was done immediately prior to experiment.

As discussed more extensively below, the apparent binding constants, K_A , we measured are $\sim 10^6$ for specific binding to CPD and $\sim 10^2$ for nonspecific binding to undamaged DNA.¹⁹ Our values are up to 3 orders of magnitude smaller than the binding constants reported earlier that were obtained through nitrocellulose filter and gel retardation assays.^{23–28} Our results are similar to those obtained from emission quenching²⁹ and surface plasmon resonance spectroscopy.³⁰ The origin of the difference appears to be the identity of the substrate: much of the earlier work used a 43 base duplex with a central CPD or the pBR322 plasmid with multiple CPDs, while the emission and surface plasmon resonance assays along with our work used short oligothymidylates with either centrally located CPD or randomly located CPD. This conclusion is tentative since we are unable to exclude any effect of the particular solvent used in the earlier studies.

We did investigate if there was any influence of MTHF on binding. Our PL, as isolated from *E. coli*, contains ~ 0.7 MTHF molecules per FAD.¹⁴ Using a previously published procedure, we titrated MTHF into PL to ensure there was 1 MTHF bound per FAD.²² We obtained binding constants for PL with stoichiometric amounts of MTHF that were indistinguishable from those obtained with PL containing substoichiometric amounts of MTHF.

Table 1. Summary of Temperature-Dependent Thermodynamics Parameters

components	temperature, K	ΔG° binding kJ/mol	ΔH° binding kJ/mol	ΔS° binding J/K mol
Ox+ssDNA	283	$-31.9 (\pm 0.7)^a$	$-21.7 (\pm 1)^b$	$+36 (\pm 5)^c$
	288	$-33.6 (\pm 0.7)$	$-26.9 (\pm 2)$	$+23 (\pm 6)$
	293	$-33.7 (\pm 0.3)$	$-31.2 (\pm 2)$	$+9 (\pm 7)$
	298	$-34.2 (\pm 0.5)$	$-37.2 (\pm 2)$	$-10 (\pm 7)$
	303	$-33.2 (\pm 1)$	$-43.2 (\pm 4)$	$-33 (\pm 10)$
Sq+ssDNA	283	$-34.1 (\pm 0.7)$	$-26.2 (\pm 2)$	$+28 (\pm 8)$
	290	$-34.3 (\pm 0.8)$	$-33.9 (\pm 2)$	$+1 (\pm 7)$
	298	$-35.1 (\pm 0.7)$	$-42.6 (\pm 5)$	$-25 (\pm 20)$
	305	$-36.3 (\pm 0.5)$	$-53.3 (\pm 3)$	$-56 (\pm 9)$
	310	$-36.7 (\pm 0.5)$	$-55.0 (\pm 4)$	$-59 (\pm 10)$
Red+ssDNA	283	$-33.3 (\pm 0.8)$	$-34.9 (\pm 2)$	$-6 (\pm 8)$
	288	$-33.6 (\pm 0.2)$	$-40.4 (\pm 0.7)$	$-24 (\pm 3)$
	293	$-34.3 (\pm 0.6)$	$-46.8 (\pm 3)$	$-43 (\pm 10)$
	298	$-34.5 (\pm 0.8)$	$-52.7 (\pm 3)$	$-61 (\pm 10)$
	303	$-34.6 (\pm 0.6)$	$-57.9 (\pm 1)$	$-77 (\pm 5)$
Ox+dsDNA	283	$-30.4 (\pm 0.7)$	$-39.6 (\pm 8)$	$-32 (\pm 30)$
	288	$-30.9 (\pm 1)$	$-47.7 (\pm 2)$	$-58 (\pm 8)$
	293	$-33.1 (\pm 0.1)$	$-51.0 (\pm 1)$	$-61 (\pm 5)$
	298	$-34.0 (\pm 0.7)$	$-54.4 (\pm 4)$	$-58 (\pm 10)$
	303	$-34.6 (\pm 0.6)$	$-50.2 (\pm 2)$	$-51 (\pm 8)$
Sq+dsDNA	283	$-32.6 (\pm 0.5)$	$-38.8 (\pm 2)$	$-22 (\pm 6)$
	290	$-33.5 (\pm 0.7)$	$-49.7 (\pm 2)$	$-56 (\pm 7)$
	298	$-35.4 (\pm 0.8)$	$-56.7 (\pm 3)$	$-71 (\pm 10)$
	305	$-35.3 (\pm 1)$	$-62.5 (\pm 2)$	$-89 (\pm 7)$
	283	$-32.6 (\pm 0.7)$	$-45.0 (\pm 5)$	$-44 (\pm 20)$
Red+dsDNA	285.5	$-33.0 (\pm 1)$	$-54.2 (\pm 6)$	$-74 (\pm 20)$
	288	$-32.9 (\pm 0.7)$	$-57.4 (\pm 3)$	$-85 (\pm 9)$
	293	$-33.4 (\pm 0.7)$	$-64.3 (\pm 5)$	$-106 (\pm 20)$
	298	$-34.6 (\pm 0.8)$	$-63.7 (\pm 4)$	$-98 (\pm 10)$
	303	$-35.0 (\pm 2)$	$-61.1 (\pm 7)$	$-86 (\pm 20)$

^a Error calculated from the standard deviation of measured K. ^b Error calculated from the standard deviation of measured values. ^c Error propagated from ΔG° and ΔH° .

Temperature Dependence of Substrate Binding. Binding of PL to damaged DNA was measured for all three oxidation states from 10 to above 30 °C, Table 1. Upon closer inspection of Table 1, one will note that although the Gibbs energy of binding is relatively unchanged with temperature, oxidation state, and substrate, the enthalpy (ΔH°) and entropy (ΔS°) are drastically affected by these parameters, as discussed further below.

The temperature dependence of the apparent enthalpy of binding (ΔH°) of PL to ssDNA is plotted in Figure 3 for all three oxidation states. It is readily apparent that the enthalpy of all of the oxidation states has the same linear dependence upon temperature in the range examined but that the value of enthalpy measured is affected by the FAD oxidation state. The fully oxidized state has the smallest binding enthalpy, while the fully reduced state has the most exothermic binding enthalpy.

Change in heat capacity,³¹ ΔC_p , is defined as the change in enthalpy of binding with temperature at constant pressure

$$\Delta C_p = (\Delta H / \Delta T)_p \quad (1)$$

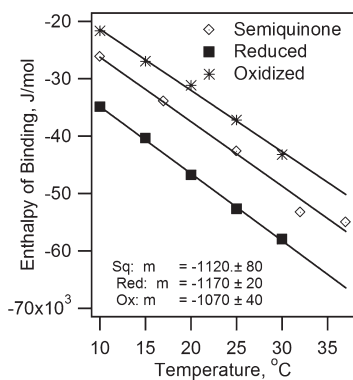


Figure 3. Temperature dependence for ssDNA binding. All experiments were completed in 20 mM potassium phosphate, 88 mM K₂SO₄, pH 7.0. Each point is the average of 3–12 individual experiments. The lines are generated from least-squares analysis, and the slopes obtained are shown.

The change in oxidation state of PL upon ssDNA binding appears to have virtually no effect on the ΔC_p ; taking into account the error calculated from least-squares analysis of the linear fits shown in Figure 3, $\Delta C_p = -1120 \text{ J/K mol}$ for all three states. As found with most DNA binding proteins, the change in heat capacity is negative.

The temperature dependence of the binding enthalpy for dsDNA is more complicated, as shown in Figure 4. The change in heat capacity for the semiquinone state is virtually unchanged from Figure 3 with $\Delta C_p = -1000 \pm 90 \text{ J/K mol}$, but the binding enthalpies for the reduced and oxidized states no longer display a linear relationship with temperature. Both enthalpies curve upward with increasing temperature; a second, endothermic process appears to be contributing to the dsDNA binding enthalpy at higher temperatures for the reduced and oxidized protein.

Salt Dependence of Substrate Binding. Studies that measure the salt dependence of substrate binding can allow one to gain insight into the specific interactions that are important between the substrate and the protein.^{32,33} An electrostatic interaction will be specifically defined as an interaction between charged groups, while the nonelectrostatic interactions are mainly van der Waals and hydrogen-bonding interactions. A recent paper by Privalov, Dragon, and Crane-Robinson³⁴ appears to validate a method that allows one to distinguish between electrostatic and nonelectrostatic interactions, as described using the following equation

$$\log K_A = \log K_{\text{nonelectrical}} - Z\psi \log[\text{Salt}] \quad (2)$$

where K_A is the observed binding constant at a specific salt concentration, $K_{\text{nonelectrical}}$ is the binding constant due only to nonelectrical interactions, Z is the number of phosphate groups that interact with the protein, and ψ is the number of cations displaced per phosphate group. The salt used is a monovalent salt (KCl in this work). There appears to be a range of values used for ψ . The work by Privalov, Dragon, and Crane-Robinson seems to indicate that $\psi = 0.70$ is reasonable for dsDNA.³⁴ Once $K_{\text{nonelectrical}}$ is obtained from this type of analysis, $\Delta G^\circ_{\text{nonelectrical}}$ and $\Delta S^\circ_{\text{nonelectrical}}$ can be calculated since it is generally assumed that there is no electrostatic contribution to the enthalpy ($\Delta H^\circ_{\text{observed}} = \Delta H^\circ_{\text{nonelectrostatic}}$), and the electrostatic component of the Gibbs energy of binding is only entropic.^{35–37} Using

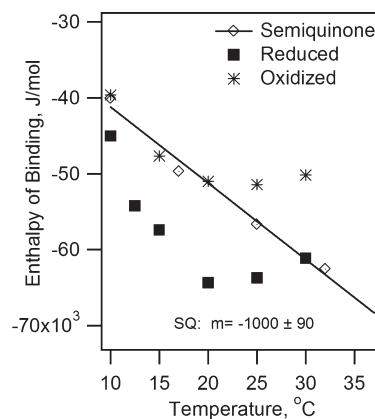


Figure 4. Temperature dependence for dsDNA binding. All experiments were completed in 20 mM potassium phosphate, 88 mM K₂SO₄, pH 7.0. Each point is the average of 3–9 individual experiments. The line is generated from least-squares analysis, and the slope obtained is shown.

this assumption, we can use the equation below to calculate the entropy of the nonelectrostatic contributions

$$\Delta G^\circ_{\text{nonelectrostatic}} = \Delta H^\circ_{\text{observed}} - T\Delta S^\circ_{\text{nonelectrostatic}} \quad (3)$$

We plotted the binding constants obtained at 25 °C as a function of salt concentration in Figures 5 (ssDNA) and 6 (dsDNA); all of our data fit well to the function described in eq 2. Using the analysis outlined above along with the assumption that the electrostatic component for the enthalpy of binding is zero, we calculated the number of phosphate contacts and the nonelectrostatic contributions to binding for each oxidation state of PL, as shown in Table 2. Included in the table are $\Delta G^\circ_{\text{total}}$ and $\Delta S^\circ_{\text{electrostatic}}$ as calculated from the data for a salt concentration of 300 mM, the same ionic strength as the buffer used in the temperature studies, to give some context for the contribution of the nonelectrical interactions to the overall free energy. The assumption that the electrostatic contribution is entirely entropic^{36,37} appears to be valid for our system since we observed no KCl dependence on our enthalpy values. The enthalpies reported in Table 2 are the average and standard deviation for the entire range of KCl data obtained for that oxidation state and substrate.

From this analysis, it appears that the number of phosphate contacts decreases for the oxidized (from 3 to 2) and reduced (from 3 to 1) states going from ssDNA to dsDNA while the semiquinone state contacts remains unchanged. The crystal structure of the complex does show interactions between the protein and one phosphate 5' to the lesion along with three phosphates 3' to the lesion; the cofactor is most likely in the fully reduced form in this structure.⁹ The discrepancy between our results and that shown in the crystal structure may originate in the heterogeneity of our dsDNA substrate.

Remarkably, although the total ΔG° (as calculated for a salt concentration of 300 mM) is virtually unchanged with both oxidation state and substrate, the components ($\Delta S^\circ_{\text{nonelectrostatic}}$ and $\Delta H^\circ_{\text{nonelectrostatic}}$) that go into ΔG° are significantly affected by the oxidation state of PL. As noted above for the temperature-dependent data, the fully reduced PL appears to have the most negative nonelectrostatic entropy.

Proton Exchange upon Substrate Binding. The number of protons lost or gained during substrate binding can be addressed

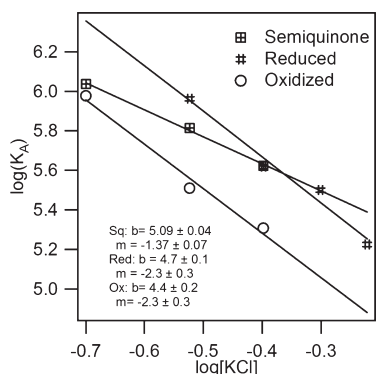


Figure 5. Salt dependence for ssDNA binding. All experiments were completed in 50 mM Hepes, pH 7.0 along with KCl at 25 °C. Each point is the average of 3–7 individual experiments. The result of the least-squares analysis for a linear fit is given for each data set.

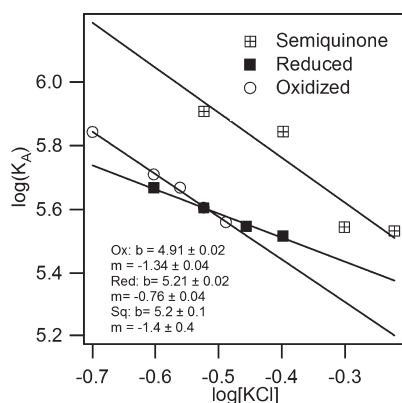


Figure 6. Salt dependence for dsDNA binding. All experiments were completed in 50 mM Hepes, pH 7.0 along with KCl at 25 °C. Each point is the average of 3–8 individual experiments. The result of the least-squares analysis for a linear fit is given for each data set.

using the approach outlined by Baker and Murphy;³⁸ the ΔH° of binding is measured at a single pH in different buffers with the resulting data fit to the following equation

$$\Delta H_{\text{observed}}^\circ = \Delta H_0 + N_{\text{H}+} \Delta H_i^{\text{buffer}} \quad (4)$$

The observed ΔH° is plotted against the buffer ionization enthalpy ($\Delta H_i^{\text{buffer}}$) to get a slope ($N_{\text{H}+}$) that corresponds to the number of protons lost (−) or gained (+). The y intercept, ΔH° , corresponds to the enthalpy of binding of the substrate for the system in a buffer with an ionization enthalpy of zero. The data are shown in the Supporting Information. Buffers of known ionization enthalpies used included potassium phosphate, Hepes, Mops, and imidazole.^{20,21} From this analysis, the fully reduced and semiquinone states appear to show identical behavior with the gain of ~1 proton with binding of ssDNA and the gain of ~0.5 proton with binding of dsDNA. The oxidized state appears to gain ~0.25 protons upon substrate binding with no discernible difference between the ssDNA and the dsDNA. Further pH studies will be done to determine the pK_a of the exchangeable proton.

DISCUSSION

We measured the enthalpy of binding over a limited temperature range to obtain the change in heat capacity of the system upon DNA binding to PL, Figures 3 and 4. The enthalpy of binding was different for each oxidation state with the fully reduced form of PL having the most exothermic heat of binding. The ΔC_p that we obtained for ssDNA binding was insensitive to the oxidation state of the FAD cofactor with a value of -1120 J/K mol obtained for all three oxidation states. The relationship between the binding enthalpy of ssDNA and temperature appeared to be quite linear over the temperature range examined. The dsDNA binding result was more complicated. The semiquinone form of PL gave virtually the same linear enthalpic behavior as observed with ssDNA and a ΔC_p of $\sim -1000 \text{ J/K mol}$, but the other two oxidation states no longer displayed a linear relationship between the enthalpy and the temperature; at least one other endothermic process is apparently contributing to the overall enthalpy of binding.

As discussed in Luque and Freire,³⁹ the observed binding enthalpy can be considered a combination of at least three terms

$$\Delta H_{\text{observed}} = \Delta H_{\text{intrinsic}} + \Delta H_{\text{conformation}} + \Delta H_{\text{protonation}} \quad (5)$$

where $\Delta H_{\text{intrinsic}}$ is the interaction between the ligand and the protein (the hydrogen bonds, van der Waals forces, solvation change). $\Delta H_{\text{intrinsic}}$ would equal $\Delta H_{\text{observed}}$ if protein and ligand have the same conformational and protonation forms in the free and bound states. The additional two terms correspond to enthalpic contributions due to conformational changes of the protein and/or ligand ($\Delta H_{\text{conformation}}$) along with any protonation or deprotonation ($\Delta H_{\text{protonation}}$) that arises upon binding. The crystal structure of the PL complexed with dsDNA appears to indicate only small, localized changes occur with the PL structure upon substrate binding; a ridge of approximately 10 amino acids is displaced by roughly 4 Å (G397 to F406 in *Anacystis nidulans*).⁹ In contrast, the crystal structure of the complex shows that the structure of the dsDNA is grossly distorted with a 50° bend along with the CPD lesion flipped out of the intrahelical base stacking.⁹ At this point, we do not have a value for the enthalpy of protonation, but it may be a minor contribution since only one proton appears to be gained. The enthalpy of binding is a fundamental thermodynamic parameter that generally describes contributions important in binding, but it is unrealistic to calculate these contributions based upon structural data. The change in heat capacity, obtained from the temperature dependence of the enthalpy, is generally used for this purpose.

Interpretation of the Change in Heat Capacity. While the individual contributions to binding enthalpies are difficult to assess, one way to gain insight into the binding process is to closely examine the change in heat capacity since dehydration of the protein surface will cause significant changes to ΔC_p . The change in heat capacity will be affected by the other contributions described in eq 5, but the extent of these contributions may be gauged by the degree of linearity of the temperature dependence for the enthalpy of binding. From the data shown in Figure 3, binding of ssDNA does not appear to have significant conformational and/or protonation contributions to the binding enthalpy since we obtain a linear relationship between enthalpy and temperature. With the exception of the semiquinone form of PL, that is not the case with the dsDNA, Figure 4. Since our

Table 2. Summary of Nonelectrostatic Interactions

components	Z	K_{nonelec}	$\Delta G^\circ_{\text{nonelec}}$ kJ/mol	$\Delta H^\circ_{\text{nonelec}}{}^a$ kJ/mol	$\Delta S^\circ_{\text{nonelec}}$ J/kmol	$\Delta S^\circ_{\text{elec}}{}^b$ J/kmol	$\Delta G^\circ_{\text{total}}{}^b$ kJ/mol
Ox+ssDNA	3.2	$2.41 (\pm 0.4) \times 10^4$	$-25.0 (\pm 0.4)^c$	$-20.9 (\pm 0.4)^d$	$14 (\pm 2)^c$	23	-31.7
Sq+ssDNA	2.0	$1.22 (\pm 0.05) \times 10^5$	$-29.0 (\pm 0.1)$	$-26.0 (\pm 1.7)$	$10 (\pm 6)$	14	-33.1
Red+ssDNA	3.3	$5.46 (\pm 0.5) \times 10^4$	$-27.0 (\pm 0.2)$	$-32.8 (\pm 3.9)$	$-20 (\pm 10)$	23	-34.0
Ox+dsDNA	1.9	$8.09 (\pm 0.4) \times 10^4$	$-28.0 (\pm 0.1)$	$-29.2 (\pm 0.9)$	$-4 (\pm 3)$	13	-32.0
Sq+dsDNA	2.0	$1.57 (\pm 0.4) \times 10^5$	$-29.6 (\pm 0.7)$	$-33.4 (\pm 3.9)$	$-13 (\pm 10)$	14	-33.9
Red+dsDNA	1.1	$1.62 (0.08) \times 10^5$	$-29.7 (\pm 0.1)$	$-46.4 (\pm 4.5)$	$-56 (\pm 20)$	8	-32.0

^a $\Delta H_{\text{electrical}} = 0$ kJ/mol.^{36, 37} ^b Calculated for [KCl] = 300 mM using least-squares analysis of data in Figures 5 and 6. ^c Errors calculated from least-squares analysis of data shown in Figures 5 and 6. ^d Error used is the standard deviation of measured values.

protonation study at pH 7.0 appears to indicate ~ 0.5 protons are gained, a conformational change to either the protein or the substrate appears to be the more likely explanation for the curvature in the enthalpy that arises at higher temperature.

While we cannot fully exclude conformational changes to the protein that may be occurring upon binding of substrate, it appears to be more likely that conformational changes to the dsDNA are the origin of the endothermic contribution observed with dsDNA. This conclusion is based upon two lines of evidence; first, there does not appear to be any protein conformational changes upon binding of ssDNA substrate, and it seems unlikely that the binding mechanism would change drastically between ssDNA and dsDNA. Second, the results of the salt study indicate that the number of phosphate contacts between the protein and the substrate decreases for the reduced and oxidized states as the substrate is changed from ssDNA to dsDNA, Table 2. The number of contacts does not change for the semiquinone state, which displays the same ΔC_p for both substrates. Therefore, it appears that our short double-stranded substrate may get slightly frayed when the protein binds, an endothermic process. This result is not surprising since the crystal structure of the complex shows the CPD lesion is flipped out of the base stacking along with a 50° bend in the dsDNA and some partial unwinding around the CPD.⁹ We did measure a melting temperature around 42°C under the buffer conditions used for the dsDNA, but it was a broadly defined transition, most likely due to the heterogeneity of the CPD location on the dsDNA.

We measured very similar changes in heat capacity for the semiquinone state of PL upon binding of either ssDNA or dsDNA, and we will use this value (-1120 to -1000 J/K mol) for further analysis of the binding site. The change in heat capacity is closely tied to changes in exposed surface area, nonpolar and polar, thus providing information on the extent and polarity of the surface that is buried upon substrate binding.^{40,41} Spolar and Record describe an empirical equation that can be used to predict ΔC_p based upon the changes in accessible surface area as DNA binds to the protein⁴¹

$$\Delta C_p = 1.34(\Delta A_{\text{nonpolar}}) - 0.586(\Delta A_{\text{polar}}) \text{ J/K mol} \quad (6)$$

In this equation, $\Delta A_{\text{nonpolar}}$ and ΔA_{polar} are the changes in nonpolar and polar accessible surface area, respectively, in units of \AA^2 . We used this empirical equation to calculate an expected ΔC_p from crystal structure data. All accessible surface areas that were calculated from the crystal and NMR structures are shown in the Supporting Information and were obtained using Surface Racer with a 1.4\AA probe.⁴² While there is not a crystal structure for the *E. coli* PL in a complex, there is for PL from *Anacystis*

nudulans with a 14-mer of duplex DNA (1TEZ, complex A);⁹ there appears to be only a $\sim 3\%$ difference in surface areas between free PL from *A. nudulans* and *E. coli*, Supporting Information. There are two crystal structures (1QNF, 1OWL) available for free PL from *A. nudulans*; we show the calculation for 1OWL since it appears to have slightly better resolution.^{7,43} Since only 10 of the 14 base pairs were resolved in the 1TEZ complex, we required the structure of a 10-mer of dsDNA with CPD for free substrate but it was difficult to find an appropriate structure. There is one crystal structure (1SMS)⁴⁴ and one NMR structure of a 10-mer with a centrally located CPD (1PIB).⁴⁵ The NMR structure is not entirely suitable since the CPD is opposite a GC mismatch. The crystal structure of the 10-mer with the central located CPD gave significantly smaller accessible surface areas (a decrease of 10–20%) than any of the NMR structures described above along with a 10-mer of undamaged DNA (1BUT)⁴⁷ and the 10-mer of DNA taken from 1TEZ (see Supporting Information). Since the data obtained from 1SMS was so anomalous to that obtained from the other structures, we excluded any further analysis of this structure. Therefore, we used the NMR structure of a 12-mer (1COC)⁴⁶ with a centrally located CPD in which we truncate the base pairs at the ends to artificially create a 10-mer. We also calculated the ΔC_p from the DNA and protein in 1TEZ; the structure was decomposed into the individual components (PL and distorted duplex DNA), and the surface areas of the individual pieces were calculated, all shown in Supporting Information. To check the integrity of the software used in the calculation of accessible surface area, we compared the amount of buried interface we calculated in the 1TEZ complex to that reported by Mees, Klar, Gnau et al., and obtain virtually the same value (1208\AA^2 compared to 1216\AA^2).⁹

The ΔC_p calculated from the changes in accessible surface area using the 1OWL PL structure, the truncated 1COC dsDNA, structure and 1TEZ for the complex was -189 J/K mol. Calculated values using the other structures described above are shown in the Supporting Information, but no calculated ΔC_p was close to that which we found experimentally ($\Delta C_p = -1120$ to -1000 J/K mol). When we repeat the same calculation using the distorted DNA structure with the flipped out CPD taken directly from the complex (1TEZ), we get $\Delta C_p = -923$ kJ/mol, very close to our experimental value. We interpret this finding to mean that PL recognizes the CPD lesion when it is exposed to the solvent; the protein does not actively flip out the CPD as part of the damage recognition mechanism. The approach we have taken has some limitations: we are using structural data from PL obtained from a different species, and we are using an empirical equation that may or may not hold for our particular system. We are also ignoring the role water molecules may play to mediate substrate binding.

Further evidence for our proposal that the enzyme recognizes a flipped out CPD comes from our experimental ΔC_p results for the ssDNA substrate. Upon the basis of optical and physical property data, oligothymidylates appear to have little base stacking in solution;^{48,49} therefore, we do not expect the UV-p(dT)₁₀ to be significantly base stacked. If the enzyme is pulling the CPD out of the base stacking in dsDNA, it seems highly unlikely that we would measure virtually identical changes in heat capacity upon binding of dsDNA and ssDNA since that additional conformational change would contribute to the overall enthalpy with a different temperature dependence.

Molecular dynamic simulations by the Wiest group provide support that recognition of the flipped out CPD by PL is plausible.^{50,51} They calculated the free energy required for a thymine dimer to undergo base flipping to be 22–31 kJ/mol; there appears to be some influence due to the bases adjacent to the dimer. Earlier calculations by Guidice found that an undamaged thymine base required a significantly higher ΔG° of 54 kJ/mol for base flipping;⁵² the barrier for base flipping of the CPD is significantly lower than what is observed for undamaged DNA, so it is more likely that the CPD spends significantly more time exposed to solvent.

It also appears we can exclude a two-step binding model in which PL binds to dsDNA in such a manner as to cause the CPD to be destabilized in the base stacking followed by a second step in which the CPD now exposed to solvent finds the binding cavity in PL. There would be three processes contributing to the overall enthalpy including dehydration of the binding surface, bending of the DNA, and binding of the CPD, making it unlikely that a linear ΔC_p for binding would be observed. The experimental design of our ITC experiments does temper this conclusion since it will be hard to see small nonlinear effects on the enthalpy over a small temperature range.

What Role Does FAD Play in Substrate Binding? A number of changes, enthalpy, electrical contacts, and proton exchange, can be detected that appear to tie into the FAD oxidation state, giving some hint of the role of the cofactor in DNA binding. The oxidized, semiquinone, and reduced states appear to make three, two, and three electrostatic contacts, respectively, with ssDNA; for simplicity, we will assume that the electrostatic contact is between a cationic group on the protein and the phosphate backbone. The semiquinone and reduced states also appear to gain one proton with ssDNA binding. In a simplistic entropic approach, it appears that the oxidized state experiences the loss of three ions, the semiquinone state has a net loss of one ion, and the reduced state has a net loss of two ions upon ssDNA binding. Since ΔS° should be more positive as more ions are lost upon substrate binding, just based upon simple ion release arguments, we would expect $\Delta S^\circ_{\text{ox}} > \Delta S^\circ_{\text{red}} > \Delta S^\circ_{\text{sq}}$. This result is similar to what we observe for $\Delta S^\circ_{\text{electrical}}$ with ssDNA where $\Delta S^\circ_{\text{ox}} \approx \Delta S^\circ_{\text{red}} > \Delta S^\circ_{\text{sq}}$, Table 2. The thermodynamic parameters obtained for the KCl buffer in Table 2 were slightly different than the parameters obtained for the K₂SO₄ buffer used in the temperature studies in Table 1, most likely due to differences in the ionization enthalpies of the buffers.

The oxidation state of the FAD controls more than the number of ions present in the binding pocket. The trend for the nonelectrostatic entropy is $\Delta S^\circ_{\text{ox}} \approx \Delta S^\circ_{\text{sq}} > \Delta S^\circ_{\text{red}}$ for both ssDNA and dsDNA, Table 2. One would expect the entropic decrease from the loss of rotational and vibrational degrees of freedom to be similar for all oxidation states of the enzyme. Therefore, two explanations are plausible for the significant

decrease in nonelectrostatic entropy observed with the fully reduced (FADH^-) state. The FADH^- state is the only oxidation state with a charge on the cofactor, and a negative charge on the cofactor may impair binding of the negatively charged substrate. Therefore, some type of shielding may be required. The shielding could arise from a change in the hydrogen-bonding network around the FAD cofactor or from addition of water molecules in close proximity to the cofactor. Using a change in entropy for water immobilization of ca. -22 J/K mol as discussed by Dragan, Frank, Liu et al.,⁵³ the measured difference in nonelectrostatic entropy of -34 (ssDNA) and -52 J/K mol (dsDNA) could be interpreted to mean that the reduced enzyme binds ~ 2 additional water molecules compared to the oxidized state. This explanation also would explain the decrease in enthalpy observed with the fully reduced state since each additional hydrogen bond would release $\sim 3 \text{ kJ/mol}$ of heat. This hypothesis is consistent with the crystal structure since there are a number of water molecules present at the interface between the protein and DNA.⁹

Use of the crystal structures of the free and complexed protein to discern if changes in the hydrogen-bonding network occur with oxidation state changes has been difficult since the flavin appears to be reduced as it is exposed to X-rays during data collection.⁴³ In *A. nidulans* PL there does appear to be a difference in the hydrogen bonding around the FAD. In free PL (1QNF), the isoalloxazine ring N3 appears to be hydrogen bound to ASP380 while O4 is hydrogen bound to ASP382.⁷ In the PL complex there is an additional hydrogen bond between NS and ASN386.⁹ The adenine ring also appears to have no hydrogen bonds in the free PL and two hydrogen bonds in the complex.^{7,9} Therefore, as noted earlier in Raman studies,¹⁴ there are changes in the hydrogen bonding around the cofactor which also may play a role in the differences observed for the entropy and enthalpy of binding with different oxidation states of PL. More extensive hydrogen bonds to the FAD cofactor would reduce the degrees of vibrational and rotational freedom of the system, causing a decrease in the observed entropy of binding in the reduced enzyme. Since the reduced state is the active state, the changes in hydrogen bonding and/or water immobilization may be important to the catalytic cycle *in vivo*.

CONCLUSIONS

Although the oxidation state of the FAD cofactor present in PL appears to have little effect on the Gibbs energy of binding, it significantly affects the enthalpy and entropy values that go into the Gibbs energy; the fully reduced state (active state) has significantly more negative entropy and enthalpy of binding. While electrostatic contributions are important and change with FAD oxidation state, most of the Gibbs contributions arise from nonelectrostatic interactions between the enzyme and the substrate. The large decrease observed for ΔH° and ΔS° found for the FADH^- state compared to the FAD_{ox} state may be due to additional binding of ~ 2 water molecules around the FAD cofactor/substrate interface and/or additional rigidity in the hydrogen bonds around the reduced FAD cofactor.

In addition, we obtained enthalpy of binding from 10 to more than 30°C for all oxidation states of PL with both ssDNA and dsDNA, and from our enthalpies, we obtained the change in heat capacity upon binding, ΔC_p . The ΔC_p was insensitive to FAD oxidation state with ssDNA binding with a value of ca. -1120 J/K mol ; virtually the same result was observed for dsDNA

binding to the semiquinone form of the enzyme. The dsDNA substrate appeared to be fraying for the reduced and oxidized enzymes since an endothermic contribution appeared at higher temperatures with dsDNA binding experiments. Using the results obtained for the semiquinone form of the *E. coli* enzyme, we compared our experimental ΔC_p value to that calculated from the accessible surface areas of existing *A. nidulans* PL and dsDNA structures in the literature. Our calculations strongly suggest that the CPD lesion is flipped out of intrahelical base stacking prior to PL binding.

■ ASSOCIATED CONTENT

Supporting Information. Additional information on calculated accessible surface areas and calculated change in heat capacity. This material is available free of charge via the Internet at <http://pubs.acs.org>.

■ AUTHOR INFORMATION

Corresponding Author

*Phone: 610-330-5824. Fax: 610-330-5355. E-mail: gindt@lafayette.edu.

Present Addresses

[†]New Jersey Dental School, 110 Bergen Street, P.O. Box 1709, Newark, New Jersey 07101, United States.

[#]Stanford University, Department of Chemistry, 380 Roth Way Keck Building 105, Stanford, California 94305, United States.

■ ACKNOWLEDGMENT

Y.M.G. is grateful for support from the National Science Foundation (CHE-0922712) and the Department of Chemistry at Lafayette College. T.W. and M.R. acknowledge support from Lafayette ARC for EXCEL Scholar funding. We gratefully acknowledge Aziz Sancar for the cell line used in this work.

■ REFERENCES

- (1) Goosen, N.; Moolenaar, G. F. *DNA Repair* **2008**, *7*, 353.
- (2) Sancar, A. *Chem. Rev.* **2003**, *103*, 2203.
- (3) Müller, M.; Carell, T. *Curr. Opin. Struct. Biol.* **2009**, *19*, 277.
- (4) Malhotra, K.; Kim, S.-T.; Walsh, C.; Sancar, A. *J. Biol. Chem.* **1992**, *267*, 15406.
- (5) Payne, G.; Sancar, A. *Biochemistry* **1990**, *29*, 7715.
- (6) Park, H.-W.; Kim, S.-T.; Sancar, A.; Deisenhofer, J. *Science* **1995**, *268*, 1866.
- (7) Tamada, T.; Kitadokoro, K.; Higuchi, Y.; Inaka, K.; Yasui, A.; de Ruiter, P. E.; Eker, A. P. M.; Miki, K. *Nat. Struct. Biol.* **1997**, *4*, 887.
- (8) Komori, H.; Masui, R.; Kuramitsu, S.; Yokoyama, S.; Shibata, T.; Inoue, Y.; Miki, K. *Proc. Natl. Acad. Sci. U.S.A.* **2001**, *98*, 13560.
- (9) Mees, A.; Klar, T.; Gnau, P.; Hennecke, U.; Eker, A. P. M.; Carrell, T.; Essen, L.-O. *Science* **2004**, *306*, 1789.
- (10) Christine, K. S.; MacFarlane, A. W.; Yang, K.; Stanley, R. J. *J. Biol. Chem.* **2002**, *277*, 38339.
- (11) Yang, W. *Cell Res.* **2008**, *18*, 184.
- (12) Friedman, J. I.; Stivers, J. T. *Biochemistry* **2010**, *49*, 4957.
- (13) Gindt, Y. M.; Schelvis, J. P. M.; Thoren, K. L.; Huang, T. H. *J. Am. Chem. Soc.* **2005**, *127*, 10472.
- (14) Schelvis, J. P. M.; Ramsey, M.; Sokolova, O.; Tavares, C.; Cecala, C.; Connell, K.; Wagner, S.; Gindt, Y. M. *J. Phys. Chem. B* **2003**, *107*, 12352–12352.
- (15) Leavitt, S.; Freire, E. *Curr. Opin. Struct. Biol.* **2001**, *11*, 560.
- (16) Privalov, P. L.; Dragon, A. I. *Biophys. Chem.* **2007**, *126*, 16.
- (17) Crane-Robinson, C.; Dragan, A. I.; Read, C. M. In *Methods in Molecular Biology*; Moss, T., Leblanc, B., Eds.; Humana Press: Totowa, NJ, 2009; Vol. 543 (DNA-Protein Interactions), p 625.
- (18) Gindt, Y. M.; Vollenbroek, E.; Westphal, K.; Sackett, H.; Sancar, A.; Babcock, G. T. *Biochemistry* **1999**, *38*, 3857.
- (19) Sokolowsky, K.; Newton, M.; Lucero, C.; Wertheim, B.; Freedman, J.; Cortazar, F.; Czochor, J.; Schelvis, J. P. M.; Gindt, Y. M. *J. Phys. Chem. B* **2010**, *114*, 7121.
- (20) Jelesarov, I.; Bosshard, H. R. *Biochemistry* **1994**, *33*, 13321.
- (21) Kozlov, A. G.; Lohman, T. M. *Biochemistry* **2006**, *45*, 5190.
- (22) Sokolova, O.; Cecala, C.; Gopal, A.; Cortazar, F.; McDowell-Buchanan, C.; Sancar, A.; Gindt, Y. M.; Schelvis, J. P. M. *Biochemistry* **2007**, *46*, 3673.
- (23) Sancar, G. B.; Smith, F. W.; Sancar, A. *Biochemistry* **1985**, *24*, 1849.
- (24) Jorns, M. S.; Sancar, G. B.; Sancar, A. *Biochemistry* **1985**, *24*, 1856.
- (25) Sancar, G. B.; Smith, F. W.; Reid, R.; Payne, G.; Levy, M.; Sancar, A. *J. Biol. Chem.* **1987**, *262*, 478.
- (26) Husain, I.; Sancar, A. *Nucleic Acids Res.* **1987**, *15*, 1109.
- (27) Kim, S. T.; Sancar, A. *Biochemistry* **1991**, *30*, 8623.
- (28) Li, Y. F.; Sancar, A. *Biochemistry* **1990**, *29*, 5698.
- (29) Jordan, S. P.; Jorns, M. S. *Biochemistry* **1988**, *27*, 8915.
- (30) Torizawa, T.; Ueda, T.; Kuramitsu, S.; Hitomi, K.; Todo, T.; Iwai, S.; Morikawa, K.; Shimada, I. *J. Biol. Chem.* **2004**, *279*, 32950.
- (31) Sturtevant, J. M. *Proc. Natl. Acad. Sci. U.S.A.* **1977**, *74*, 2236.
- (32) Crane-Robinson, C.; Dragan, A. I.; Privalov, P. L. *Trends Biochem. Sci.* **2006**, *31*, 547.
- (33) Ladbury, J. E.; Williams, M. A. *Protein Rev.* **2007**, *5*, 231.
- (34) Privalov, P. L.; Dragan, A. I.; Crane-Robinson, C. *Nucleic Acids Res.* **2011**, *39*, 2483.
- (35) Manning, G. S. *Q. Rev. Biophys.* **1978**, *11*, 179.
- (36) Record, M. T., Jr.; Lohman, T. M.; de Haseth, P. J. *Mol. Biol.* **1976**, *107*, 145.
- (37) de Haseth, P. L.; Lohman, T. M.; Record, M. T., Jr. *Biochemistry* **1977**, *16*, 4783.
- (38) Baker, B. M.; Murphy, K. P. *Biophys. J.* **1996**, *71*, 2049.
- (39) Luque, I.; Freire, E. *Proteins: Struct., Funct., Genet.* **2002**, *49*, 181.
- (40) Ha, J.-H.; Spolar, R. S.; Record, M. T. *J. Mol. Biol.* **1989**, *209*, 801.
- (41) Spolar, R. S.; Record, M. T., Jr. *Science* **1994**, *263*, 777.
- (42) Tsodikov, O. V.; Record, M. T.; Sergeev, Y. V. *J. Comput. Chem.* **2002**, *23*, 600.
- (43) Kort, R.; Komori, H.; Adachi, S.; Miki, K.; Eker, A. *Acta Crystallogr., Sect. D: Biol.* **2004**, *D60*, 1205.
- (44) Park, H.; Zhang, K.; Ren, Y.; Nadji, S.; Sinha, N.; Taylor, J.-S.; Kang, C. *Proc. Natl. Acad. Sci. U.S.A.* **2002**, *99*, 15965.
- (45) Lee, J.-H.; Park, C.-J.; Shin, J.-S.; Ikegami, T.; Akutsu, H.; Choi, B.-S. *Nucleic Acids Res.* **2004**, *32*, 2474.
- (46) McAtee, K.; Jing, Y.; Kao, J.; Taylor, J.-S.; Kennedy, M. A. *J. Mol. Biol.* **1998**, *282*, 1013.
- (47) Dornberger, U.; Flemming, J.; Fritzsch, H. *J. Mol. Biol.* **1998**, *284*, 1453.
- (48) Riley, M.; Maling, B.; Chamberlin, M. J. *J. Mol. Biol.* **1966**, *20*, 359.
- (49) Ts'o, P. O.; Rapaport, S. A.; Bollum, F. J. *Biochemistry* **1966**, *5*, 4153.
- (50) O'Neil, L. L.; Grossfield, A.; Wiest, O. *J. Phys. Chem. B* **2007**, *111*, 11843.
- (51) O'Neil, L. L.; Wiest, O. *J. Phys. Chem. B* **2008**, *112*, 4113.
- (52) Giudice, E.; Varnai, P.; Lavery, R. *ChemPhysChem* **2001**, *2*, 673.
- (53) Dragan, A. I.; Frank, L.; Liu, Y.; Makeyeva, E. N.; Crane-Robinson, C.; Privalov, P. L. *J. Mol. Biol.* **2004**, *343*, 865.